International Journal of Biological Macromolecules 208 (2022) 475–485

Contents lists available at ScienceDirect

International Journal of Biological Macromolecules

journal homepage: www.elsevier.com/locate/ijbiomac

Sodium alginate-*f*-GO composite hydrogels for tissue regeneration and antitumor applications

Muhammad Umar Aslam Khan [a,b,*], Saiful Izwan Abd Razak [c,d], Sajjad Haider [e], Hafiz Abdul Mannan [f], Javed Hussain [g], Anarwul Hasan [a,b]

[a] Department of Mechanical and Industrial Engineering, Qatar University, Doha 2713, Qatar.
[b] Biomedical Research Center, Qatar University, Doha 2713, Qatar
[c] BioInspired Device and Tissue Engineering Research Group, School of Biomedical Engineering and Health Sciences, Faculty of Engineering, Universiti Teknologi Malaysia, 81300 Skudai, Johor, Malaysia.
[d] Centre for Advanced Composite Materials, Universiti Teknologi Malaysia Skudai, Johor Malaysia.
[e] Department of Chemical Engineering, College of Engineering, King Saud University, PO Box 800, Riyadh 11421, Saudi Arabia.
[f] Institute of Polymer and Textile Engineering, University of Punjab, Quaid-e-Azam Campus, Lahore 54590, Pakistan.
[g] National Center for Physics, Quaid-i-Azam University Islamabad Campus, Islamabad 44000, Pakistan.

ARTICLE INFO

Keywords:
Antibacterial
Antitumor
Drug release kinetics
Biopolymers
Tissue regeneration

ABSTRACT

Biopolymer-based composite hydrogels have attracted tremendous attention for tissue regeneration and antitumor applications. Since sodium alginate is a biopolymer, they offer excellent therapeutic options with long-term drug release and low side effects. To prepare multifunctional composite hydrogels with anticancer and tissue regeneration capabilities, sodium alginate (SA) and graphene oxide (GO) were covalently linked and crosslinked with tetraethyl orthosilicate (TEOS) by the solvothermal method. The structural and morphological results show that the hydrogels exhibit the desired functionality and porosity. The swelling of hydrogels in an aqueous and PBS medium was investigated. SGT-4 had the highest swelling in both aqueous and PBS media. Swelling and biodegradation of the hydrogel were inversely related. The drug release of SGT-4 was determined in different pH media (pH 6.4, 7.4, and 8.4) and the kinetics of drug release was determined according to the Higuchi model (R2 = 0.93587). Antibacterial activities were evaluated against severe infectious agents. Uppsala (*U87*) and osteoblast (*MC3T3-E1*) cell lines were used to determine the anticancer and biocompatibility of the composite hydrogels, respectively. These results suggest that the composite hydrogels could be used as potential biomaterials for tissue regeneration and antitumor applications.

1. Introduction

A brain tumor (glioma) is the best-known life-threatening tumor. Even after surgery, radiation, and chemotherapeutic treatment, the majority of patients with glioma die within 2 years of diagnosis [1]. An immense amount of work is being done on the treatment and care of glioma tumors. Many researchers have used two-dimensional (2D) cell culture systems to assess tumor cell sensitivity to radiotherapy and chemotherapy and to guide clinical treatments [2]. Meningitis has been reported in some postoperative procedures. Meningitis is an inflammation of the protective membranes covering the brain and spinal cord, which is usually caused by a bacterial infection following cranial surgery that requires immediate recognition and treatment. Such infections have also been reported in bone regeneration studies. In postoperative meningitis, the patient can only be treated with antibiotics [3]. The convenience of self-administration, precise location, low dose, and systemic toxicity all contribute to the therapeutic impact [4]. Various nanocarriers, such as liposomes, nanovesicles, and nanoemulsions have been studied to improve drug absorption through the skin surface to overcome these limitation [5,6]. Composite hydrogels have special structures and surface roughness similar to those of tissues and also natural extracellular matrix. Composite hydrogels have been identified as carriers for the treatment of cancer, but they have the disadvantage that their therapeutic agents leak and aggregate over a long period of time [7–9]. To prevent this process, the composite hydrogels can be coated with polymers to achieve the desired release kinetics. Hydrogels

* Corresponding author at: Biomedical Research Center, Qatar University, Doha 2713, Qatar.
E-mail address: umar007khan@gmail.com (M.U.A. Khan).

https://doi.org/10.1016/j.ijbiomac.2022.03.091
Received 13 January 2022; Received in revised form 28 February 2022; Accepted 15 March 2022
Available online 19 March 2022

produced from biopolymers are suitable for biological systems and are environmentally compatible. [10,11]. Alginates are a form of biological macromolecules that have attracted great interest in biomedical applications due to their antioxidant, bioactive, and biocompatible properties. They are used in tissue engineering, wound healing, drug delivery, film production, and in the preparation of a number of other biomaterials. In various studies, alginates have been reported to be anticancer, analgesic, hemostatic, nontoxic, highly biocompatible, and allergenic biomaterials [12,13]. The synthetically produced biopolymers have low mechanical properties. They should have more mechanical properties to maintain their structural integrity, hold more and retain biofluid to facilitate vascularization and regeneration of wounds [14,15]. Various scientific studies have shown that polysaccharides with GO-based hydrogels have excellent antibacterial, antiviral, antifungal, antitumor, anticarcinogenic, and antidiabetic activities [16,17].

Graphene-based materials have attracted the attention of scientists because they are easier to modify. Graphene oxide (GO) is enriched with numerous functional groups such as carboxyl and hydroxyl groups. GO is biocompatible and has been used to develop various biomaterials for different biomedical applications, such as targeted drug delivery, treatment, tissue engineering, gene delivery, *etc.* [18]. The specific toxicity of graphene on cancer cells could be an advantage. Several scientific studies have shown that graphene can act as an anticancer agent in the fight against the spread of cancer. Moreover, various anticancer drugs can be bound to the graphene surface to be used in cancer therapy [19].

In this study, we report a novel multifunctional composite hydrogel for the treatment of brain tumors. Sodium alginate was functionalized with GO *via* the solvothermal method and crosslinked with tetraethyl orthosilicate (TEOS) to fabricate composite hydrogels. The structure, surface morphology, and hydrophilicity were investigated by Fourier transform infrared spectroscopy (FTIR), scanning electron microscope (SEM), and contact angle conducted, respectively. Swelling and biodegradation analyses were performed at different pHs values to determine the pH-dependent behavior of the composite hydrogels. We used silver sulfadiazine as a model drug to study its release *in vitro* using Franz transdermal diffusion method. Antibacterial activities were evaluated against severe infections with Gram-positive and Gram-negative pathogens. *In-vitro* biocompatibility studies were performed using Uppsala (*U87*) and osteoblast (*MC3T3-E1*) cell lines to analyze the biocompatible and anticancer activities of the composite hydrogels. The produced multifunctional composite hydrogels would not only be a potential step forward in the treatment wounds during regeneration but also in treating brain tumor.

2. Materials and methods

2.1. Materials

Sodium alginate (biopolymer), TEOS (crosslinker), GO (filler), PBS solution, HCl, and NaOH were purchased from Sigma Aldrich. All the chemicals were of analytical grade and were used as received.

3. Methods

3.1. Preparation of polymeric composite hydrogels

The hydrothermal method was used to synthesize composite hydrogels. Briefly, GO (0.03 mg) and sodium alginate (2 g) were placed in a 50 mL stainless steel autoclave and allowed to stand for 25 min. The autoclave was then kept in an oven at 50 °C for 12 h to allow the reaction of the polymer and GO. The autoclave was removed from the oven and cooled to obtain the composite gel. The obtained gel was dispersed in a 25 mL distilled water in a beaker *via* stirring and at 55 °C for 1 h. Then, different concentrations of TEOS (100, 150, 200, and 250 μL) were dissolved in methanol (5 mL) and added dropwise to the whorl of the polymer suspension and stirred for 3 h. Due to the different concentrations of the crosslinker, the samples were assigned the codes STG-1, STG-2, STG-3 and, STG-4. The liquid form of the prepared multifunctional composite hydrogels was packed in Teflon eppendorfs for biological assays. The proposed chemical reaction of the composite gel is shown in Scheme 1. The mixed solutions of the multifunctional composite hydrogel were poured into Petri dishes dried under vacuum at 50 °C for 24 h to form porous hydrogels. The films of the well-dried multifunctional composite hydrogel were peeled off from the Petri dishes and packed in a polyethylene bag for further analysis. The proposed chemical reaction of the crosslinked multifunctional composite hydrogel is shown in a Scheme 2.

3.2. Drug loading and transdermal drug delivery

Silver sulfadiazine is a well-known antibacterial drug. 20 mg of it was accurately weighed and completely dissolved in 5 mL of ethanol. Then, it was added dropwise to the whorl of the polymeric composite system (SA-GO) with constant stirring for 2 h to obtain a homogenized mixture of drug and SA-GO suspension. After 2 h of stirring, 200 μL of crosslinker dissolved in 5 mL of ethanol was added dropwise to the suspension. The suspension was stirred for another 3 h at 60 °C. In accordance with previous reported method, the Franz diffusion method was used to determine the release of the drug in PBS media (pH 6.4, 7.4, and 8.4) at 37 °C [20]. Every 10 min, 5 mL of the sample solution was run through a double beam UV–vis spectrophotometer to determine the *in vitro* drug release. PBS media served as the reference standard, and *in vitro* drug release analysis was presented using calibration curve.

4. Characterization

4.1. Fourier-transform infrared spectroscopy

FTIR spectroscopy (Nicolet 5700, Waltham, MA, USA) was used to investigate the functionalities of the composite hydrogels. The KBr pellet of the composite hydrogels were prepared with a hydraulic press. The spectra were recorded in the range of 4000 to 400 cm^{-1} with 150 routine scans.

4.2. Scanning electron microscopy

Morphological analysis of the composite hydrogels was performed using SEM microscope (JSM-6701S). The well dried composite hydrogels were coated with gold and fixed to the chamber with magnetic tape and the micrographs were taken.

4.3. Swelling analysis

The swelling analysis of composite hydrogels was determined at different pH values in aqueous and PBS media to estimate their swelling behavior. The well-dried composite hydrogels were cut into a square shape and carefully weighed (50 mg) as initial weight (W_i). The composite hydrogels were soaked in aqueous and PBS media with different pH values (1−13) at room temperature. The composite hydrogels were removed from the media after a set period and weighed as a final weight (W_f). The excess surface solvent was carefully removed with filter paper before weighing the hydrogels. The swelling percentage was calculated using Eq. (1).

$$Swelling\ (\%) = \frac{W_f - W_i}{W_i} \times 100 \quad (1)$$

whereas, W_f = final weight of composite hydrogels, W_i = initial weight of composite hydrogels.

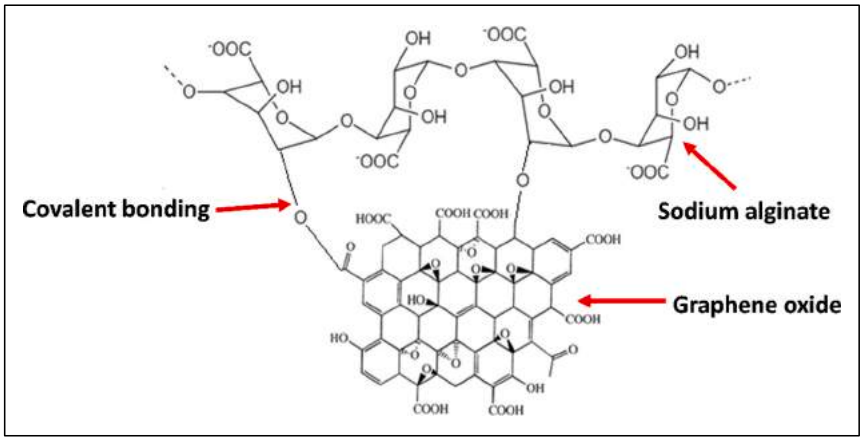

Scheme 1. The proposed reaction of sodium alginate and GO *via* the solvothermal method to prepare composite gel.

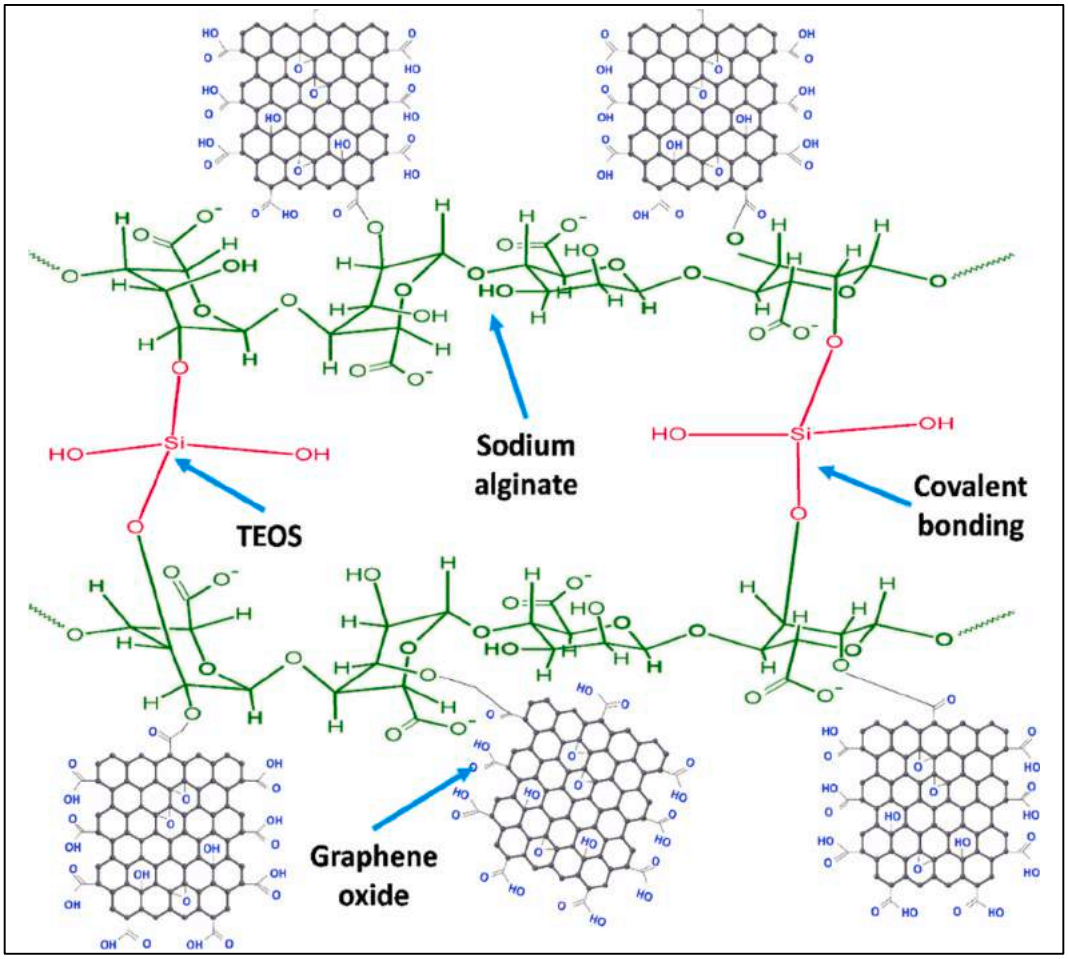

Scheme 2. The proposed chemical reaction/crosslinking of multifunctional composite hydrogel *via* blending using TEOS crosslinker.

4.4. Biodegradation

The well-dried hydrogels were cut into a square shape and carefully weighed (50 mg) and immersed in PBS media under *in vitro* conditions (pH 7.4 at 37 °C) for different periods of time. The weight of the hydrogel was recorded before and after biodegradation study and the weight loss of hydrogel was calculated by Eq.2.

$$Weight\ loss\ (\%) = \frac{W_i - W_t}{W_i} \times 100 \quad (2)$$

where: $\boldsymbol{W_i}$ = initial weight of the hydrogel, $\boldsymbol{W_t}$ = weight of hydrogel at a time "t".

4.5. Wetting analysis

The wetting behavior of the multifunctional composite hydrogel was

investigated using the water contact angle technique to determine the hydrophobicity and hydrophilicity of the composite hydrogels. The water contact angle analysis system (JY-82, Dingsheng, Chengde, China) was used to study the wetting properties of the hydrogels.

4.6. In vitro studies

4.6.1. Drug release kinetics

The release kinetics of silver sulfadiazine were studied using zero-order, first-order, Hixson-Crowell, Korsmeyer-Peppas, Higuchi, and Baker-Lonsdale mathematical models. The release data from Franz diffusion at different pH was applied to following Eqs. (3)–(8).

$$\text{Zero}-\text{order } M_t = M_o + K_o t \tag{3}$$

$$\text{First order } logC = logC_o - \frac{kt}{2.303} \tag{4}$$

$$\text{Higuchi model } ft = Q = K_H \times t^{1/2} \tag{5}$$

$$\text{Hixson Crowell model } W^{1/3} - W^{1/3} = kt \tag{6}$$

$$\text{Korsmeyer}-\text{Peppas model } ln\frac{M_t}{M_o} = n\ lnt + lnK \tag{7}$$

$$\text{Baker}-\text{Lonsdale model } F_t = \frac{2}{3}\left[1-\left(1-\frac{M_t}{M_o}\right)^{\frac{2}{3}}\right]\frac{M_t}{M_o} = K(t)^{0.5} \tag{8}$$

where, *Mt* = drug release amount at "*t*" time, *KH*, *K*, and *Ko* are constants.

4.6.2. Antibacterial activity

The disc diffusion method was used to determine the antibacterial potential of these composite hydrogels against the Gram-positive and Gram-negative bacterial strains (*Staphylococcus aureus* (*S. aureus*), *Escherichia coli* (*E. coli*), and *Pseudomonas aeruginosa* (*P. aeruginosa*)). An equal amount of the molten agar was poured into Petri plates for solidification. The Gram-positive and Gram-negative bacterial strains were spread on the solidified agar using a glass spreader. Then, 90 μL of the multifunctional composite hydrogel was added to the Petri plates and incubated at 37 °C for 12 h. The antibacterial activity of the composite hydrogels was determined by measuring the zones of inhibition (mm).

4.6.3. Anticancer activity

MTT assays were used to test the anticancer activity of the composite hydrogels against U-87 (aggressive cancer cell) cell lines. These cells were cultured at 37 °C for 24 h in Dulbecco's Modified Eagle Medium [(DMEM) (10% PBS and 1% penicillin-streptomycin solution)]. When cultures reached the desired confluence, 10,000 cells were added to each well of a 96-well culture plate and incubated for 24 h under standard *in vitro* conditions (5% CO_2, 37 °C, and 90% humidity). Composite hydrogels and solvent control were added to the 96-well culture plate at a final volume of 200 μL per well and incubated for an additional 24 h. The plates were then inoculated with MTT (15 μL) in each well and incubated at 37 °C for 3 h until intracellular purple formazan crystals were visible under the microscope. The MTT solution was removed with the solubilization solution (150 μL DMSO). The plate was covered with foil to protect it from light, and absorbance was immediately measured with a spectrophotometer at 550 nm. The experiment was performed in triplicate and the results are the average of the three experiments.

4.6.4. Cell viability and proliferation

Cytotoxicity and cell proliferation as a function of concentrations (from 1.0 to 2.5 μg/mL) of the composite hydrogel were determined by cell viability and optical density of *MC3T3-E1* cell lines. After different time intervals (24, 48, and 72 h), cell viability and proliferation were measured. The gelatin-coated well-plate was used as a positive control and incubated under standard *in vitro* conditions. The cell-cultured plates were incubated again for 2 h in neutral red (NR) medium (40 μg/mL) according to the NR method of Repetto [21]. Cells were stained with a staining solution after washing off the excess NR medium with PBS medium. Absorbance was measured at 540 nm using a microplate reader to determine optical density, and cells viability was calculated using Eq. 9.

$$Cell\ vaibility = \frac{OD_s}{OD_c} \times 100 \tag{9}$$

where: OD_s = sample optical density, OD_c = control optical density.

4.6.5. Cell culture and morphology

Approximately 5000 cells/cm^2 were cultured in each well of a 24 well plate at various time intervals under standard *in vitro* conditions (37 °C, 5% CO2, 90% humidity). An inverted microscope (Nikon Eclipse TS100) was used to view cell culture and morphology.

4.6.6. Cell culture and adherence SEM analysis

SEM was used to examine the surface morphology and cell adhesion of composite hydrogels (JEOL-JSM-6480). *MC3T3-E1* cell lines were cultured on composite hydrogels after different time intervals (24, 48, and 72 h). To remove nonadherent cells, the multifunctional composite hydrogel cultured with cells were washed in PBS solution. The hydrogel with adherent cells was then fixed in absolute ethanol for 5 min at room temperature. The multifunctional composite hydrogel films were thoroughly dried, and cell adhesion was assessed using SEM. Morphological analysis was performed at a voltage of 5 kV, an operating pressure of 7 $\times 10^{-2}$ bar, and a deposition current of 20 mA for 2.0 min.

4.7. Statistical analysis

SPSS software was used to perform the statistical analyses. The mean and standard deviation were used to present all data. Except for cell morphology, all analyses were performed in triplicate ($n = 3$), and statistical significance was set at $P < 0.05$.

5. Results and discussions

5.1. Structural analysis

The FT-IR spectra of the composite hydrogels are shown in Fig. 1, with detailed positioning of the vibrational bands. The broadband from 3600 to 3200 cm^{-1} was attributed to O—H functional groups originating from the crosslinker (TEOS), the biopolymer (SA), and the filler (GO). The broadband also explains the intera-molecular and inter-molecular H-bonding due to free or bonded O—H groups of SA, GO, TEOS. The vibrational bands at 2918 and 2846 cm^{-1} are stretching vibrations of C—H [22,23]. The vibrational bands at 1647, 1574 cm^{-1} are attributed to C═O and COOH functional groups. The bands at 1543, 1471, and 1419 cm^{-1} are the characteristic bands of GO [24,25]. The vibrational bands from 1110 to 1000 cm^{-1} are asymmetric stretching vibrations of –Si–O–C and –Si–O–Si, attributed to TEOS. The TEOS vibration bands that merged with GO-bonded polysaccharides, confirmed the successful cross-linking of the hydrogel. The vibrational bands at 1149 and 894 cm^{-1} are the characteristic bands of polysaccharides. These bands were assigned to saccharine and pyranose rings, respectively [23,26]. The presence of the characteristic bands of all components of the composite hydrogel in the FT-IR spectral profile successfully confirmed the preparation of a multifunctional composite hydrogel.

5.2. Morphological analysis

The interconnected porosity and pore size play an important role in

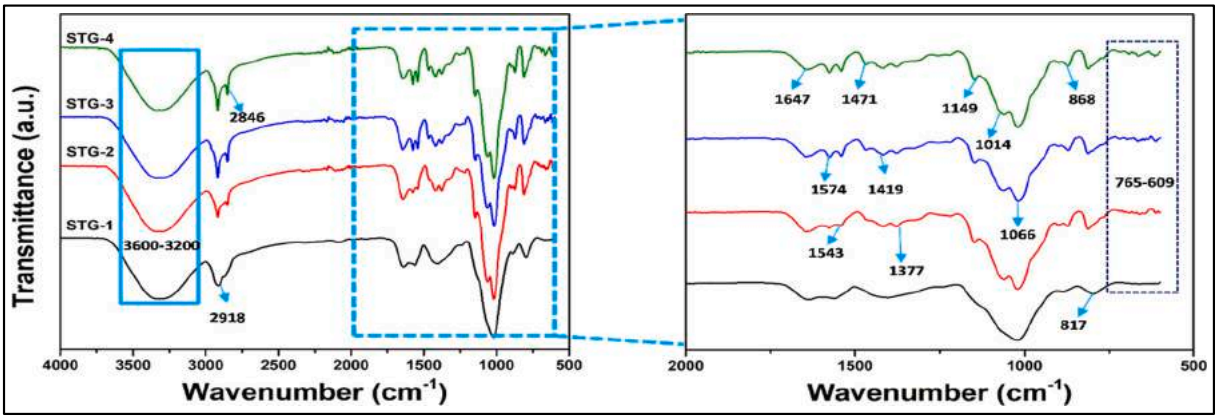

Fig. 1. FTIR spectrum of the multifunctional composite hydrogel.

biological processes such as cell growth and penetration into a extracellular matrix, diffusion of nutrients, gas exchange (oxygen/carbon dioxide), and exchange of waste materials during wound healing [23,27]. Therefore, one of the most important properties of hydrogels is their porous nature, which allows cells to pass through and retains biofluids. Fig. 2 shows the SEM micrographs of composite hydrogels. The composite hydrogels exhibit uniform pore distribution, micropores, and well-connected porosity. Successful crosslinking facilitates retention and swelling of the biofluid and results in interconnected porosity. Due to the available OH groups, increasing TEOS concentration increases H-bonding (as shown in structural analysis (Fig. 1)). Increased crosslinking increases structural integrity and interconnected porosity, and ensures that the multifunctional composite hydrogels maintain their structural integrity during interaction with biofluids (plasma, wound exudate and blood, *etc.*). Therefore, composite hydrogels with porous morphology are considered effective biomaterials that support cell adhesion, migration, and controlled release of drugs [23,26]. Thus, the porous morphology of multifunctional composite hydrogels confirms the successful crosslinking and preparation of composite hydrogels.

5.3. Swelling analysis

The ability to swell is an essential property of hydrogels. When they come into contact with biofluids, the biofluids penetrate the polymeric network of the hydrogel through pores and surface functional groups. The pores begin to expand, allowing more solvent molecules to penetrate the hydrogel network. The hydrophilic functionalities on the polymer backbone give the hydrogels the ability to absorb water, while the cross-links between the network chains give the hydrogels the ability to resist uncontrolled biodegradation. To achieve swelling equilibrium, the expanding and retracting forces must balance each other [23]. The pores of the polymeric network rapidly fill with biofluids during the swelling process and expand as the biomaterial swells. This pore expansion facilitates cell migration and diffusion of nutrients. The affinity of the polymer chains and their functionalities enable the uptake of biofluid molecules by the hydrogel network [28]. Therefore, it is assumed that the solvation of the polymer network chains, their functionalities, and the filling of the pores by the solvent determines the uptake of the biofluid by the hydrogel in equilibrium.

To determine the behavior of the polymer network chains and their functionalities during swelling, we studied the swelling of the composite hydrogels in PBS and aqueous media at different pH values (1–13). (Fig. 3 (a and b)). The multifunctional composite hydrogel swelled more when the pH was changed from acidic to neutral (pH 1 to 7) and swelled less when the pH was changed from neutral to basic (pH 7 to 13). This behavior of the composite hydrogels is attributed to the changes in the functionalities of the polymer network. SA has several functional groups (as shown in Scheme 1 and 2) and OH is common to these functionalities. In acidic environments (pH < 7), the high H+ concentration leads to protonation of all OH group-bearing functionalities in the composite hydrogel. This leads to minimal H-bonding between the molecules of the biofluid and the functionalities of the composite hydrogel. Therefore,

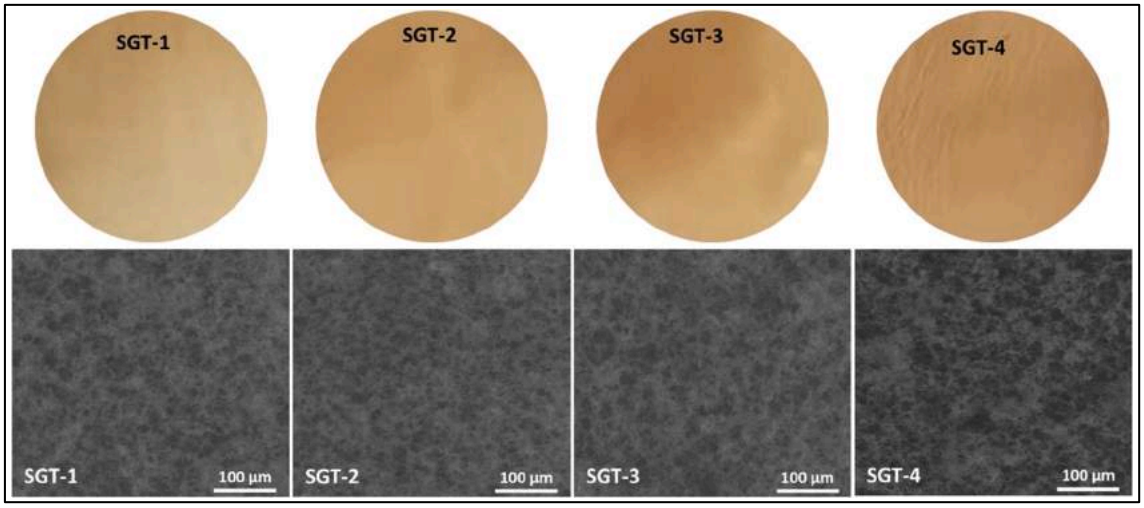

Fig. 2. Surface morphology of composite hydrogel.

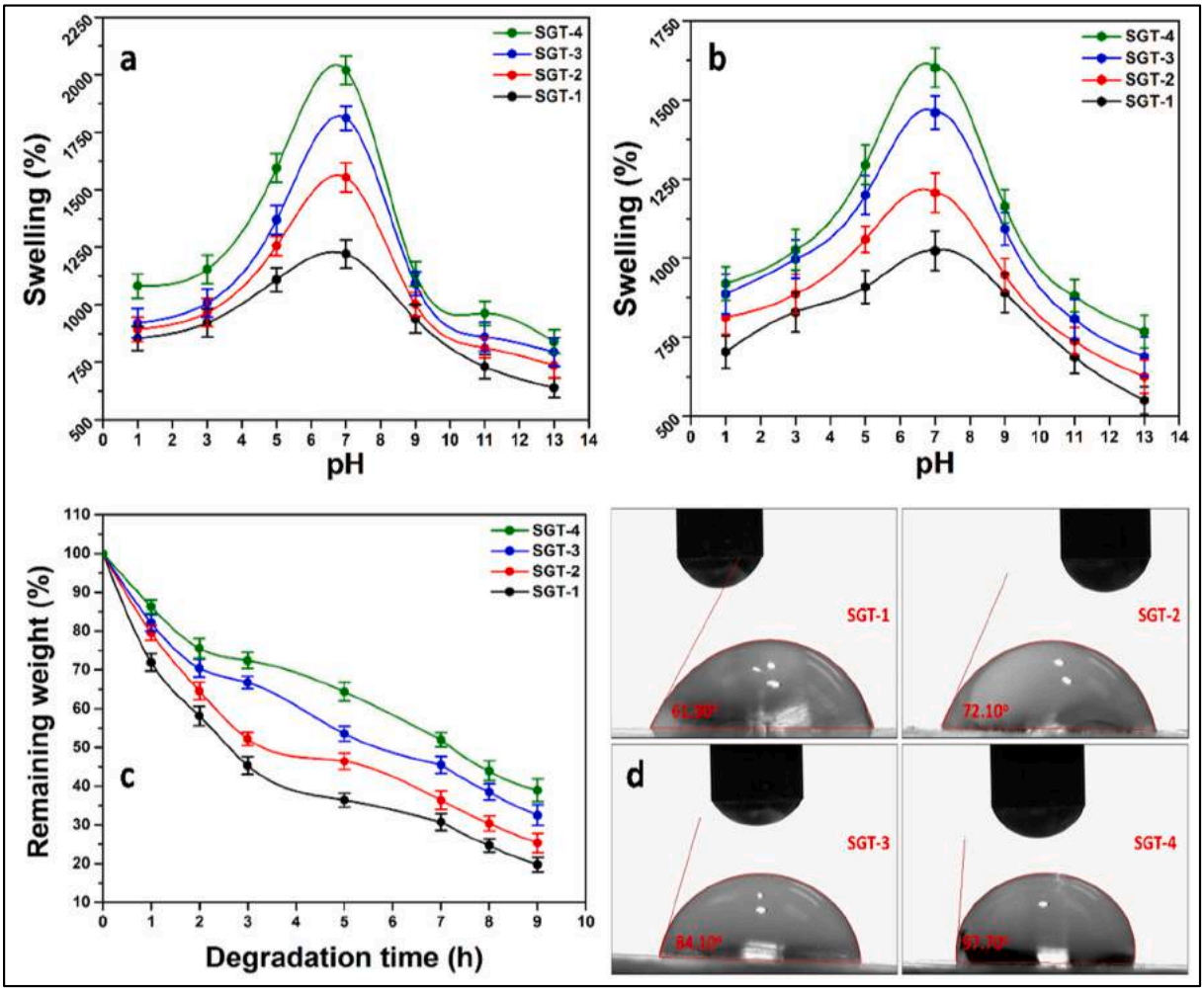

Fig. 3. Swelling analysis of composite hydrogels under different pH in PBS (a) and (b) aqueous media, (c) biodegradation in PBS buffer media, and (d) wetting behavior.

the composite hydrogel showed minimal swelling in acidic environments. In a neutral environment (pH 7), the concentration of H+ ions is lower. All OH-bearing functionalities of the composite hydrogel tend to form hydrogen bonds with the molecules of the biofluid. Therefore, the maximum swelling is observed in a neutral environment [29]. In a basic environment (pH > 7), dissociation of the OH functionalities to negatively charged species occurs. This leads to an increased movement of mobile ions, and thus in a decrease in osmotic pressure. The decrease in osmotic pressure resulted in less swelling. It is also worth noting that an increase in TEOS concentration resulted in increased swelling. This is attributed to an increase in functional groups -OH, which also contribute to the formation of hydrogen bonds. Since optimal crosslinking leads to structural integrity and uniformly distributed porosity, SGT-1 therefore shows lower swelling, while SGT-3 and SGT-4 show the highest swelling. Consequently, the different swelling behavior confirms the successful crosslinking at different TEOS concentrations.

5.4. Biodegradation analysis

Biodegrdation is a crucial phenomenon. Biodegrdation is important in controlled dissolution of the biomaterials that support cell adhesion and proliferation. The subspecies produced during biodegrdation do not cause host reactions or side effects. The biodegradation of composite hydrogels, which are largely composed of SA, can be explained by the breaking of the bonds between SA, GO, and TEOS (Fig. 3c). The glycosidic linkages between the units of the SA can be easily broken. These chains can be further degraded by metabolic pathways [30]. However, the degradation of the SA can be controlled by crosslinker or filler. Fig. 3c shows the biodegradation behavior of the composite hydrogels with different TEOS concentrations. SGT-1 exhibits the highest biodegradability and SGT-4 the lowest. Also SGT-1 exhibits a rapid degradation rate, while SGT-4 shows a continuous degradation behavior. The delayed and lowest degrdation of the SGT-4 is attributed to the higher concentration of the crosslinker. [31]. The differential biodegradability confirms the successful crosslinking of the composite hydrogels at different TEOS concentrations.

5.5. Wetting analysis

The hydrophilicity and hydrophobicity of biomaterials are determined by their wetting behavior, which contributes to the optimization of the material for better cell adhesion and proliferation. Water uptake occurs in composite hydrogels due to the presence of water-loving functional groups attached to the polymeric backbone. H-bonding is favoured by these functional groups. Fig. 3d shows the wetting behavior of the composite hydrogels (at 0 s: SGT-1 = 61.90 ± 4.9°, SGT-3 = 61.84 ± 10° and SGT-4 = 97.70 ± 3.8°). It can be seen that the hydrophilic behavior shifts towards hydrophobicity with increasing TEOS concentration, which can be attributed to the close packing of the hydrogel network [8]. The composite hydrogel SGT-1 exhibits hydrophilicity and the composite hydrogels SGT-3 and SGT-4 exhibits hydrophobicity, which can be attributed to the increasing degree of crosslinking. The

change in hydrophilicity of the composite hydrogels confirms the successful crosslinking of the composite hydrogel by TEOS. GO also plays an important role in crosslinking *via* weak attractive forces (van der Waal, π-π stacking and lone pair, *etc.*) due to multiple available functional groups [32]. The stronger swelling of the multifunctional composite hydrogel (SGT-4) might be related to the lower degradation rate and more OH functionalities compared to SGT-1. Measuring the weight of the sample before and after swelling plays an important role in determining the swelling values. Thus, an increased degradation rate results in a lower weight of SGT-1 compared to SGT-3 and SGT-4 during swelling in the same time interval. The lower weight of SGT-1 could lead to lower swelling. However, the hydrophilicity can be further optimized by changing the time and TEOS concentration. The different hydrophilic and hydrophobic behaviours confirm the successful preparation and crosslinking of the multifunctional composite hydrogel with different TEOS concentrations.

5.6. *In vitro studies*

5.6.1. *Drug release analysis*

As shown in Fig. 4, we selected SGT-4 to study its drug release behavior in PBS media as a function of time (due to its optimized physicochemical properties). Different release behavior of silver sulfadiazine was observed in slightly acidic and basic (pH 6.4 and 8.4), and in neutral (pH 7.4) PBS media. In neutral media, a minimum release of 11.19% was observed after 2 h and a maximum release of 89.32% was observed after 36 h. Drug release was continuous and uniform drug release was observed after 24 h, which could be due to equilibrium. The continuous drug release is attributed to the breakdown of intermolecular and week van der Waals interactions of the drug with the composite hydrogels (GO, TEOS, and SA) [6]. Erosion, diffusion, and swelling are three different mechanisms by which the drug is released. In the erosion mechanism, a hydrolytic process, the polymeric system begins to degrade from the edges. In the presence of biofluids, diffusion then occurs in the polymer matrix due to a difference in concentration. The diffusion is directly responsible for the swelling of the composite hydrogels [33]. As shown in Fig. 4, the release of silver sulfadiazine is continuous in all pH media, indicating a smooth and continuous degradation and swelling of the composite hydrogels. The 72 h period is critical for the sustained and controlled release of the drug, because several dangerous pathogens can attack open and fresh wounds, and the body's self-defense mechanisms need time to develop. To combat pathogens that cause severe infections in wounds, a controlled and sustained release of drugs is essential. Failure to maintain a sustained and controlled drug release may result in toxic or ineffective wound care and treatment [6]. From the result (Fig. 4), the composite hydrogel developed by our group showed sustained and continuous drug release under different of pH values, indicating that it could be used for wound treatment.

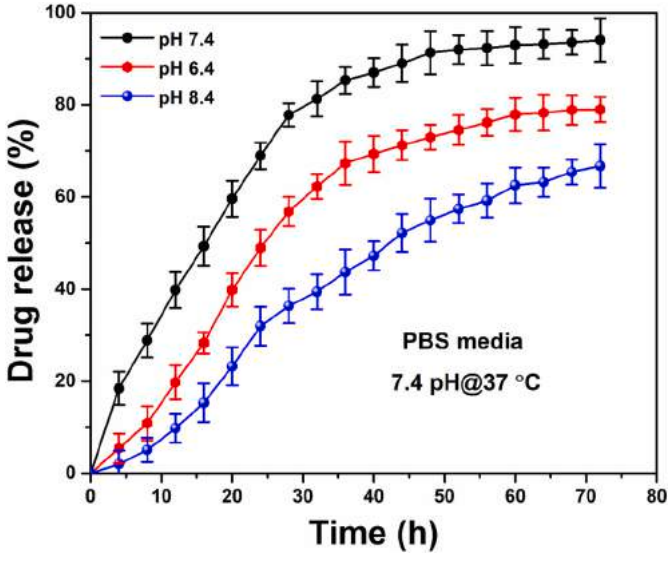

Fig. 4. The drug release profile presents the drug release behavior under acidic (pH = 6.4), neutral (pH = 7.4) and basic (pH = 8.4) media.

5.6.2. *Drug release kinetics*

Advances in materials design and engineering have led to the rapid development of innovative biomaterials of increasing complexity that target desired applications. Both nondegradable and degradable polymers are being used extensively in the field of controlled delivery. Studying the kinetics of drug release can help us understand how material systems work. The gap between the macroscopic data and the release mechanism needs to be bridged. To study the release mechanism and structure-function relationship of a material system, researchers must first understand the drug release behavior at the molecular level [34]. To better understand the drug release mechanism, we used different mathematical fitting models for drug release in neutral medium (zero-order, 1st order, Higuchi, Peppas, Hixson, and Baker-Lonsdale models), as shown in Fig. 5. The first-order regression coefficient was calculated to be 0.7884, which is not a good fit compared to other models with regression coefficient $R^2 >$ of 0.9368, such as the Higuchi model. These models appear to be ideal for controlled and consistent drug delivery. The diffusion exponent "n" of the Korsmeyer-Peppas model explains non-Fickian drug transport from multifunctional composite hydrogels (Eq. (7)). Non-Fickian drug transport is present when $0.45 < n < 0.89$ [6]. Table 1 summarizes the statistical parameters (intercept, slope, and R^2) of the models. The Higuchi model fits better than the other models. The release of the drug from a polymer matrix is explained by the Higuchi model. This model is based on the hypotheses that (i) the initial drug concentration in the matrix is much higher than the solubility of the drug; (ii) the diffusion of the drug occurs only in one dimension (the edge effect is negligible); (iii) the drug particles are smaller than the thickness of the system; (iv) the swelling and dissolution of the matrix are negligible; (v) the diffusivity of the drug is constant, and (vi) perfect sink conditions exist in the release environment [35].Our material is a polymeric matrix that releases the drug in a controlled and sustained manner. This is critical for preventing infections without causing toxicity or delayed release of the drug, as shown by the best model fit.

5.6.3. *Antimicrobial activities*

The disc diffusion method was used to investigate the antibacterial activities of the composite hydrogels against various bacteria. As shown in Fig. 6a, the antibacterial activities were measured in terms of inhibition zones, and it was found that each sample exhibited different bacterial activities. Due to the increased functionality, the multifunctional composite hydrogel (SGT-1) has the lowest antibacterial activity and the multifunctional composite hydrogel (SGT-4) has the highest antibacterial activity. These composite hydrogels have the highest antibacterial activity against *S. aureus* and the lowest against *P. aeruginosa*, which may be due to a polysaccharide-phospholipid-lipopolysaccharide interaction. Since lipopolysaccharides have a higher negative surface charge and the polymeric part of the hydrogel has multiple functional groups, it is more effective [36,37]. These functional groups can attach to the bacterial membrane and thus bacterial growth. Another possibility is that the polymeric component interacts with bacterial DNA, preventing it from being used for translation and transcription. Sharp-edged-GO, on the other hand, can rupture bacterial membranes and destroy the bacterial structure because they have a large their high surface area, surface charge, multiple functional groups, and π–π stacking with sharp edges [38]. These functional groups can interact with the bacterial membrane and transfer their charges, which hinders bacterial growth. Therefore, these composite hydrogels

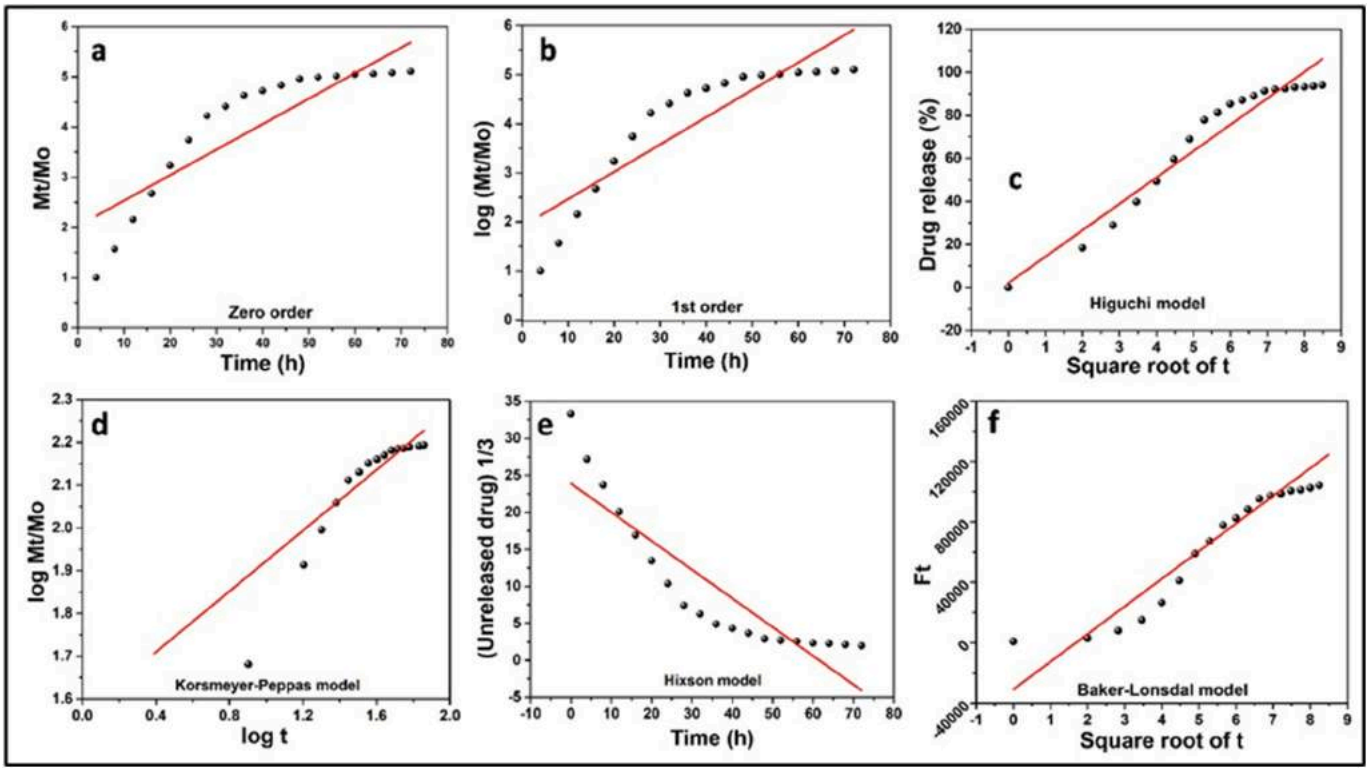

Fig. 5. The drug release kinetic in neutral media (pH 7.4) of SGT-3 against different mathematical fitting models (a) zero-order, (b) 1st order, (c) Higuchi model, (d) Peppas model (e) Hixson model, and (f) Baker-Lonsdale model.

Table. 1
Summarizes the intercept, slope, and regression coefficient values.

Models	Intercept	Slop	R^2
Zero-order	2.02539 ± 0.27601	0.0508 ± 0.00572	0.78769
First Order	1.90699 ± 0.30073	0.05571 ± 0.00695	0.7884
Higuchi model	2.06056 ± 4.53116	12.26271 ± 0.75519	0.93587
Korsmeyer-Peppas model	1.56769 ± 0.07691	0.35514 ± 0.05091	0.74867
Hixon Crowell model	23.89947 ± 1.96287	−0.38851 ± 0.04658	0.79209
Baker-Lonsdale model	−30,879.63862 ± 18,287.94637	18,287.54537 ± 1808.94637	0.849

can interact with bacterial cells to control DNA transformation. Therefore, the multifunctional composite hydrogels could be potential biomaterials for wound care and treatment with enhanced antibacterial activity.

5.6.4. Anticancer/cytotoxic activities

The anticancer activities of all hydrogels at different intervals are shown in Fig. 6b. The composite hydrogels showed different anticancer activities after different periods. The anticancer activity of these hydrogels was highest after 72 h of incubation. The sharp edge of the GO may rapture the cellular membrane and the polymeric hydrogel after penetrating the cell may take control of the nucleus to prevent cell proliferation and cause cell death. The morphology of the cells may also change from an elongated to spherical [39]. Furthermore, the increasing contact time of the multifunctional composite hydrogel also causes anticancer activities [40]. The results show that the composite hydrogels initially supported cell viability and later their behavior changed into anticancer [41]. This trend can be attributed to the optimal crosslinking, polymeric, and GO interaction with cells. The composite hydrogels are therefore considered to have anticancer potential

5.6.5. Cell viability and proliferation

The biocompatible behavior of the composite hydrogels was evaluated by measuring cell viability and proliferation against *MC3T3-E1* cell lines. (Fig. 7 (a and b)). Due to the different crosslinking behavior, these composite hydrogels exhibit different cell viability and proliferation. It is critical for tissue regeneration that the biomaterial supports cell viability and proliferation. With increasing time intervals, the *MC3T3-E1* cell line showed the desired cell viability and proliferation. After 72 h, the composite hydrogels exhibited the highest cell viability and proliferation. Due to the different functionality and physicochemical phenomena, the composite hydrogels promoted biocompatibility, which will support tissue regeneration. SGT-4 exhibited the highest cell viability and proliferation and SGT-1 the lowest, as shown in Fig. 8a and b. This might be due to wetting behavior, surface morphology of the composite hydrogel, and the combined effects of SA, GO, and TEOS.

5.6.6. Cell adherence

Cell adhesion morphology was studied by culturing *MC3T3-E1* and Uppsala (*U87*) cell lines on the multifunctional composite hydrogels and taking microscopic images with SEM. Both cell lines exhibited different growth rates and morphologies (Fig. 8.). The *MC3T3-E1* line grew slowly and formed cell clusters initially, but showed proper cell morphology

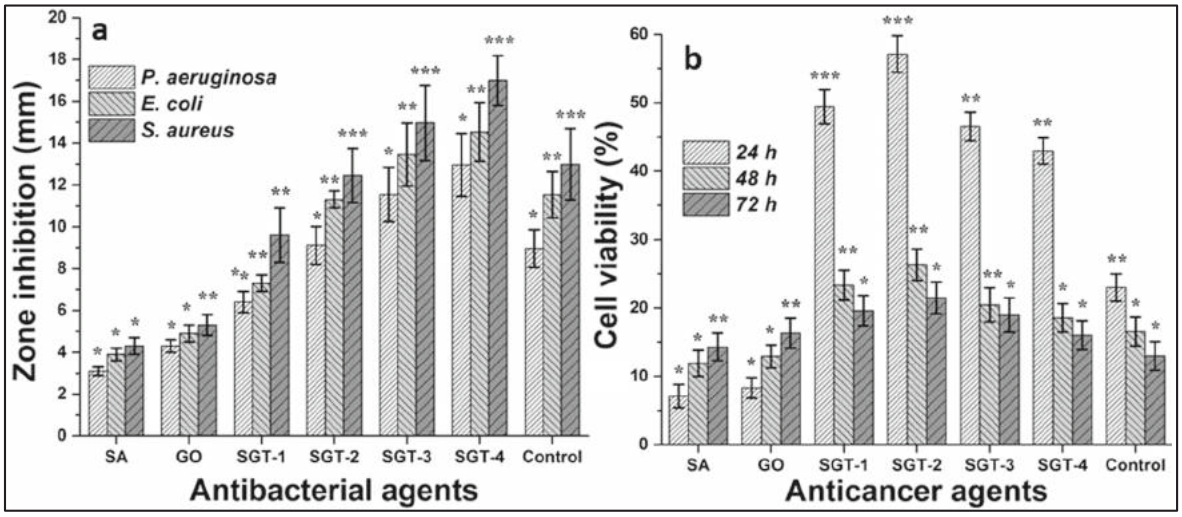

Fig. 6. (a) The bar graph shows antibacterial activities and (b) anticancer activity of composite hydrogels at different intervals against *U87* cell lines. The control for the antibacterial study is Alcohol. Whereas the anticancer study is Dimethyl sulfoxide (DMSO).

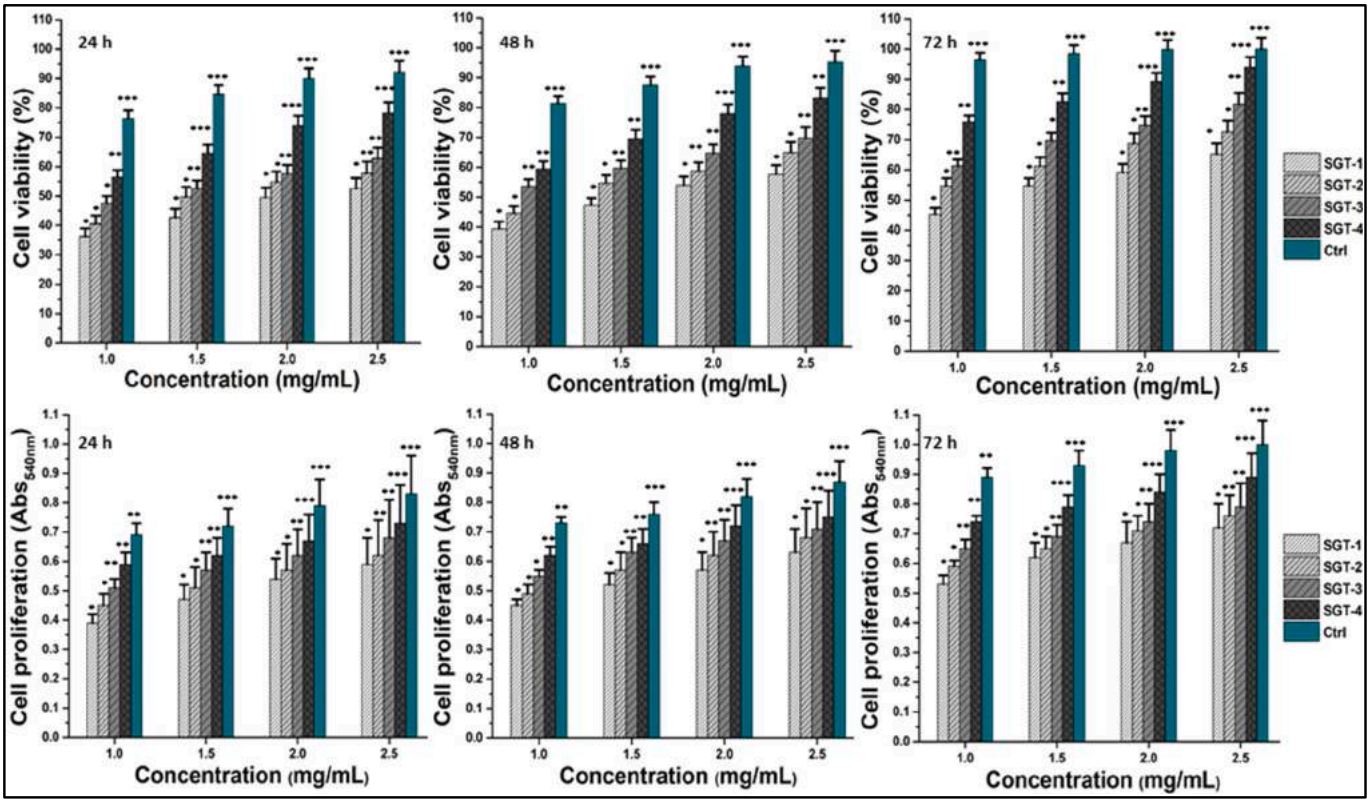

Fig. 7. The cell viability (a) and proliferation (b) using *MC3T3-E1* cell lines at different periods (24, 48, and 72 h) to determine the biocompatibility of composite hydrogels. The calculated significance values were (cell viability) $p < 0.001$ and was (optical density) $p < 0.05$.

and maximal cells after 72 h and at SGT-4. The yellow arrows show cell clusters, whereas the red arrow represents a single cell. In contrast, the *U87* cells initially grew faster; they were larger, had longer protrusions, and formed spheroids (the cells of the *U87* lineage stuck closely together and filled empty spaces [42] with a high density at SGT-2. However, the growth of the cells at SGT-4 is not only reduced, but also the cell morphology changes from elongated to spherical. These changes in morphology indicate that the cells were initially able to adhere to the composite hydrogel and proliferate, but were later killed (apoptosis). Similar results can also be found in the literature [39,43]. The results show that STG-4 has the highest adhesion for *MC3T3-E1* cell line and the lowest for *U87* cell line after 72 h. This may be due to the optimal crosslinking and surface functionality that promotes adhesion of *MC3T3-E1* cell line and killing of *U87* cell line.

6. Conclusion

In this study, we prepared multifunctional composite hydrogels using SA, GO, and TEOS. The structural, morphological, physicochemical, drug-releasing, antibacterial, anticancer, and biocompatibility

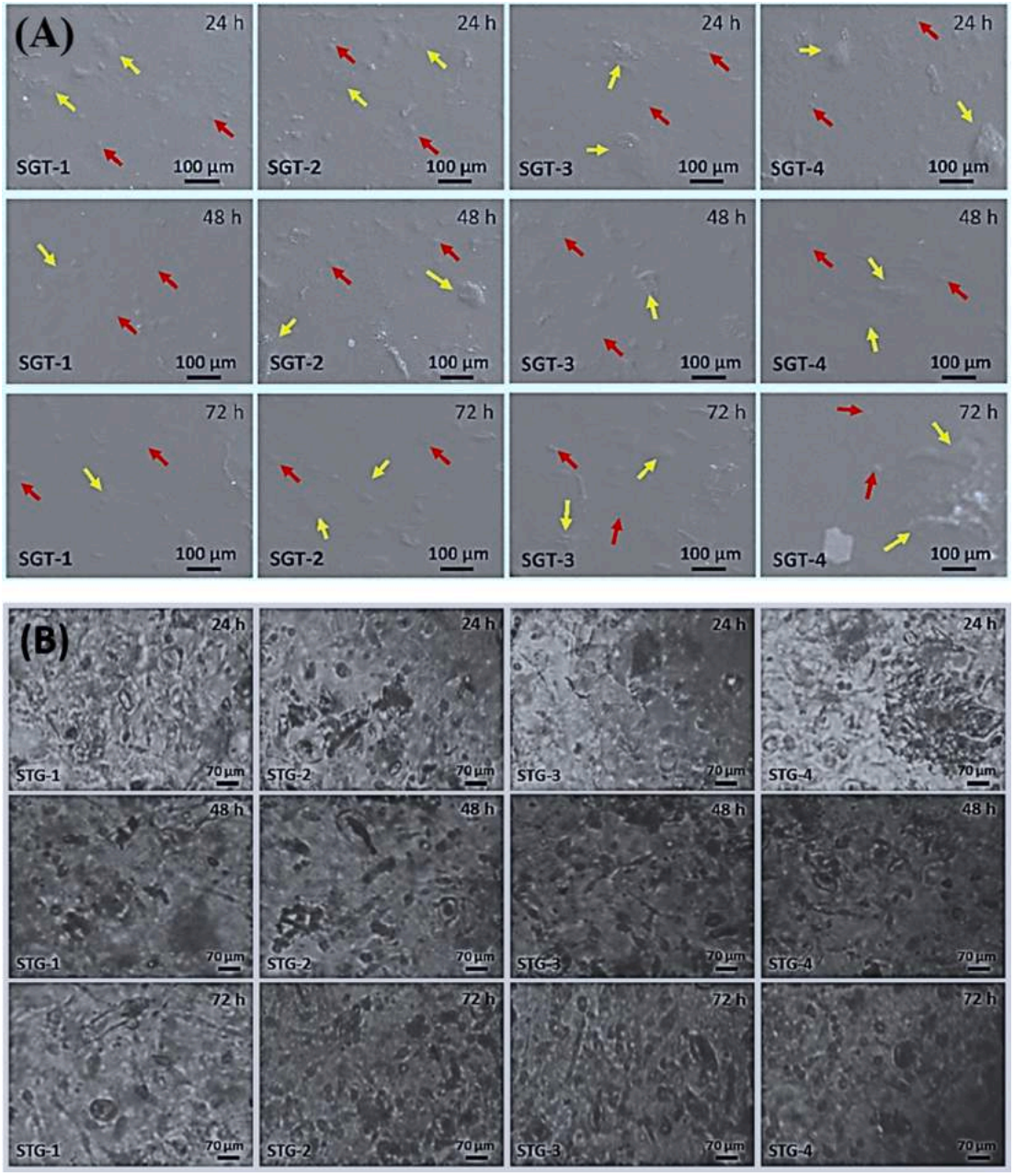

Fig. 8. Cell morphology of against composite hydrogels at various time intervals (24, 48, and 72 h) (A) osteoblast (*MC3T3-E1*) and (B) Uppsala (*U87*). The red-arrows show cell adherence and yellow arrows indicate cell adherence in cell cluster formation. (For interpretation of the references to colour in this figure legend, the reader is referred to the web version of this article.)

studies were thoroughly investigated. We investigated the effects of crosslinking and found that increasing the TEOS concentration improved the structural, functional, drug-releasing, antibacterial, anticancer, and biocompatible effects of the composite hydrogel. The composite hydrogels respond to pH as they swell and release drugs under different pH media. The multifunctional composite hydrogel (SGT-4) was found to be an optimized formulation with significant structural, morphological, physicochemical, and biological properties. Therefore, the prepared multifunctional composite hydrogel could be a potential biomaterial for tissue regeneration and antitumor applications.

CRediT authorship contribution statement

Conceptualization, Muhammad Umar Aslam Khan; **Data acquisition,** Muhammad Umar Aslam Khan and Hafiz Abdul Mannan; **Formal analysis,** Muhammad Umar Aslam Khan, Javed Hussain and Sajjad Haider; **Funding acquisition,** Muhammad Umar Aslam Khan and Saiful Izwan Abd Razak; **Methodology,** Muhammad Umar Aslam Khan and Sajjad Haider; **Project administration,** Muhammad Umar Aslam Khan, Saiful Izwan Abd Razak, and Anwarul Hasan; **Resources,** Muhammad Umar Aslam Khan, and Saiful Izwan Abd Razak; **Software,** Muhammad Umar Aslam Khan and Javed Hussain; **Supervision,** Muhammad Umar Aslam Khan and Saiful Izwan Abd Razak; **Validation:** Saiful Izwan Abd Razak, Sajjad Haider, and Anwarul Hasan; **Visualization,** Muhammad Umar Aslam Khan; **Writing–original draft,** Muhammad Umar Aslam Khan; **Writing – review & editing,** Muhammad Umar Aslam Khan and Sajjad Haider.

Declaration of competing interest

The authors declare no conflict of interest.

Data availability

Data will be made available on request.

Acknowledgment

This article was made possible by the NPRP12S-0310-190276 grant funded by Qatar National Research Fund (a part of Qatar Foundation). The statements made here are the sole responsibility of the authors.

References

[1] F. Hanif, K. Muzaffar, K. Perveen, S.M. Malhi, S.U. Simjee, Glioblastoma multiforme: a review of its epidemiology and pathogenesis through clinical presentation and treatment, Asian Pac. J. Cancer Prev. 18 (1) (2017) 3.
[2] C.J. Jiglaire, N. Baeza-Kallee, E. Denicolaï, D. Barets, P. Metellus, L. Padovani, O. Chinot, D. Figarella-Branger, C. Fernandez, Ex vivo cultures of glioblastoma in three-dimensional hydrogel maintain the original tumor growth behavior and are suitable for preclinical drug and radiation sensitivity screening, Exp. Cell Res. 321 (2) (2014) 99–108.
[3] S.R. Dashti, H. Baharvahdat, R.F. Spetzler, E. Sauvageau, S.W. Chang, M.F. Stiefel, M.S. Park, N.C. Bambakidis, Operative intracranial infection following craniotomy, Neurosurg. Focus. 24 (6) (2008) E10.
[4] T. Haque, K.M. Rahman, D.E. Thurston, J. Hadgraft, M.E. Lane, Topical therapies for skin cancer and actinic keratosis, Eur. J. Pharm. Sci. 77 (2015) 279–289.
[5] Y. Liang, Z. Li, Y. Huang, R. Yu, B. Guo, Dual-dynamic-bond cross-linked antibacterial adhesive hydrogel sealants with on-demand removability for post-wound-closure and infected wound healing, ACS Nano 15 (4) (2021) 7078–7093.
[6] S. Nazir, M.U.A. Khan, W.S. Al-Arjan, S.I. Abd Razak, A. Javed, M.R.A. Kadir, Nanocomposite hydrogels for melanoma skin cancer care and treatment: in-vitro drug delivery, drug release kinetics and anti-cancer activities, Arab. J. Chem. 14 (5) (2021), 103120.
[7] B. Dhandayuthapani, Y. Yoshida, T. Maekawa, D.S. Kumar, Polymeric scaffolds in tissue engineering application: a review, Int. J. Polym. Sci. 2011 (2011).
[8] M.U.A. Khan, I. Iqbal, M.N.M. Ansari, S.I.A. Razak, M.A. Raza, A. Sajjad, F. Jabeen, M. Riduan Mohamad, N. Jusoh, Development of antibacterial, degradable and pH-responsive chitosan/guar gum/polyvinyl alcohol blended hydrogels for wound dressing, Molecules 26 (19) (2021) 5937.
[9] M.U.A. Khan, Z. Yaqoob, M.N.M. Ansari, S.I.A. Razak, M.A. Raza, A. Sajjad, S. Haider, F.M. Busra, Chitosan/poly vinyl alcohol/graphene oxide based pH-responsive composite hydrogel films: drug release, anti-microbial and cell viability studies, Polymers 13 (18) (2021) 3124.
[10] M.B. Applegate, J. Coburn, B.P. Partlow, J.E. Moreau, J.P. Mondia, B. Marelli, D. L. Kaplan, F.G. Omenetto, Laser-based three-dimensional multiscale micropatterning of biocompatible hydrogels for customized tissue engineering scaffolds, Proc. Natl. Acad. Sci. 112 (39) (2015) 12052–12057.
[11] Z. Deng, R. Yu, B. Guo, Stimuli-responsive conductive hydrogels: design, properties, and applications, Mater. Chem. Front. 5 (5) (2021) 2092–2123.
[12] A.K. Azad, S.M.A. Al-Mahmood, J.F. Kennedy, B. Chatterjee, H. Bera, Electro-hydrodynamic assisted synthesis of lecithin-stabilized peppermint oil-loaded alginate microbeads for intestinal drug delivery, Int. J. Biol. Macromol. 185 (2021) 861–875.
[13] L. Fan, Y. Du, B. Zhang, J. Yang, J. Zhou, J.F. Kennedy, Preparation and properties of alginate/carboxymethyl chitosan blend fibers, Carbohydr. Polym. 65 (4) (2006) 447–452.
[14] M.U. Aslam Khan, H. Mehboob, S.I. Abd Razak, M.Y. Yahya, A.H. Mohd Yusof, M. H. Ramlee, T.J. Sahaya Anand, R. Hassan, A. Aziz, R. Amin, Development of polymeric nanocomposite (Xyloglucan-co-methacrylic acid/hydroxyapatite/SiO2) scaffold for bone tissue engineering applications—in-vitro antibacterial, cytotoxicity and cell culture evaluation, Polymers 12 (6) (2020) 1238.
[15] K. Hu, M.K. Gupta, D.D. Kulkarni, V.V. Tsukruk, Ultra-robust graphene oxide-silk fibroin nanocomposite membranes, Adv. Mater. 25 (16) (2013) 2301–2307.
[16] M.I. Hussain, M. Farooq, Q.A. Syed, Nutritional and biological characteristics of the date palm fruit (Phoenix dactylifera L.)–a review, Food Biosci. (2019), 100509.
[17] Q. Wang, X. Hu, Y. Du, J.F. Kennedy, Alginate/starch blend fibers and their properties for drug controlled release, Carbohydr. Polym. 82 (3) (2010) 842–847.
[18] H. Shen, L. Zhang, M. Liu, Z. Zhang, Biomedical applications of graphene, Theranostics 2 (3) (2012) 283.
[19] S.R. Shin, Y.-C. Li, H.L. Jang, P. Khoshakhlagh, M. Akbari, A. Nasajpour, Y. S. Zhang, A. Tamayol, A. Khademhosseini, Graphene-based materials for tissue engineering, Adv. Drug Deliv. Rev. 105 (2016) 255–274.
[20] S. Sa'adon, S.I.A. Razak, K. Fakhruddin, Drug-loaded poly-vinyl alcohol electrospun nanofibers for transdermal drug delivery: review on factors affecting the drug release, Procedia Comput. Sci. 158 (2019) 436–442.
[21] G. Repetto, A. Del Peso, J.L. Zurita, Neutral red uptake assay for the estimation of cell viability/cytotoxicity, Nat. Protoc. 3 (7) (2008) 1125–1131.
[22] M.U.A. Khan, M.A. Al-Thebaiti, M.U. Hashmi, S. Aftab, S.I. Abd Razak, S. Abu Hassan, A. Kadir, M. Rafiq, R. Amin, Synthesis of silver-coated bioactive nanocomposite scaffolds based on grafted beta-glucan/hydroxyapatite via freeze-drying method: anti-microbial and biocompatibility evaluation for bone tissue engineering, Materials 13 (4) (2020) 971.
[23] M.U.A. Khan, S. Haider, M.A. Raza, S.A. Shah, S.I. Abd Razak, M.R.A. Kadir, F. Subhan, A. Haider, Smart and pH-sensitive rGO/arabinoxylan/chitosan composite for wound dressing: in-vitro drug delivery, antibacterial activity, and biological activities, Int. J. Biol. Macromol. 192 (2021) 820–831.
[24] C. Valencia, C.H. Valencia, F. Zuluaga, M.E. Valencia, J.H. Mina, C.D. Grande-Tovar, Synthesis and application of scaffolds of chitosan-graphene oxide by the freeze-drying method for tissue regeneration, Molecules 23 (10) (2018) 2651.
[25] P.S. Selvamani, J.J. Vijaya, L.J. Kennedy, B. Saravanakumar, N.C.S. Selvam, P. J. Sophia, Facile microwave synthesis of cerium oxide@ molybdenum di-sulphide@ reduced graphene oxide ternary composites as high performance supercapacitor electrode, J. Electroanal. Chem. 895 (2021), 115401.
[26] M.U.A. Khan, M.A. Raza, S.I.A. Razak, M.R. Abdul Kadir, A. Haider, S.A. Shah, A. H. Mohd Yusof, S. Haider, I. Shakir, S. Aftab, Novel functional antimicrobial and biocompatible arabinoxylan/guar gum hydrogel for skin wound dressing applications, J. Tissue Eng. Regen. Med. 14 (10) (2020) 1488–1501.
[27] M. Li, Y. Liang, Y. Liang, G. Pan, B. Guo, Injectable stretchable self-healing dual dynamic network hydrogel as adhesive anti-oxidant wound dressing for photothermal clearance of bacteria and promoting wound healing of MRSA infected motion wounds, Chem. Eng. J. 427 (2022), 132039.
[28] G. Chitra, D. Franklin, S. Sudarsan, M. Sakthivel, S. Guhanathan, Indole-3-acetic acid/diol based pH-sensitive biological macromolecule for antibacterial, antifungal and antioxidant applications, Int. J. Biol. Macromol. 95 (2017) 363–375.
[29] Y. Zhao, H. Su, L. Fang, T. Tan, Superabsorbent hydrogels from poly (aspartic acid) with salt-, temperature-and pH-responsiveness properties, Polymer 46 (14) (2005) 5368–5376.
[30] Y. Hong, H. Song, Y. Gong, Z. Mao, C. Gao, J. Shen, Covalently crosslinked chitosan hydrogel: properties of in vitro degradation and chondrocyte encapsulation, Acta Biomater. 3 (1) (2007) 23–31.
[31] R.A. McBath, D.A. Shipp, Swelling and degradation of hydrogels synthesized with degradable poly (β-amino ester) crosslinkers, Polym. Chem. 1 (6) (2010) 860–865.
[32] L. Liang, P.C. Rieke, J. Liu, G.E. Fryxell, J.S. Young, M.H. Engelhard, K.L. Alford, Surfaces with reversible hydrophilic/hydrophobic characteristics on cross-linked poly (N-isopropylacrylamide) hydrogels, Langmuir 16 (21) (2000) 8016–8023.
[33] M.U.A. Khan, S.I.A. Razaq, H. Mehboob, S. Rehman, W.S. Al-Arjan, R. Amin, Antibacterial and hemocompatible pH-responsive hydrogel for skin wound healing application:in vitro drug release, Polymers 13 (21) (2021) 3703.
[34] Y. Fu, W.J. Kao, Drug release kinetics and transport mechanisms of non-degradable and degradable polymeric delivery systems, Expert. Opin. Drug Deliv. 7 (4) (2010) 429–444.
[35] S. Dash, P.N. Murthy, L. Nath, P. Chowdhury, Kinetic modeling on drug release from controlled drug delivery systems, Acta Pol. Pharm. 67 (3) (2010) 217–223.
[36] T. Dai, C. Wang, Y. Wang, W. Xu, J. Hu, Y. Cheng, A nanocomposite hydrogel with potent and broad-spectrum antibacterial activity, ACS Appl. Mater. Interfaces 10 (17) (2018) 15163–15173.
[37] J. Qu, X. Zhao, P.X. Ma, B. Guo, Injectable antibacterial conductive hydrogels with dual response to an electric field and pH for localized "smart" drug release, Acta Biomater. 72 (2018) 55–69.
[38] M.U.A. Khan, S.I. Abd Razak, H. Mehboob, M.R. Abdul Kadir, T.J.S. Anand, F. Inam, S.A. Shah, M.E. Abdel-Haliem, R. Amin, Synthesis and characterization of silver-coated polymeric scaffolds for bone tissue engineering: antibacterial and in vitro evaluation of cytotoxicity and biocompatibility, ACSOmega 6 (6) (2021) 4335–4346.
[39] L. Ou, S. Lin, B. Song, J. Liu, R. Lai, L. Shao, The mechanisms of graphene-based materials-induced programmed cell death: a review of apoptosis, autophagy, and programmed necrosis, Int. J. Nanomedicine 12 (2017) 6633.
[40] A. Kumari, S.K. Yadav, S.C. Yadav, Biodegradable polymeric nanoparticles based drug delivery systems, Colloids Surf. B: Biointerfaces 75 (1) (2010) 1–18.
[41] K. Santhosh, M.D. Modak, P. Paik, Graphene oxide for biomedical applications, J. Nanomed. Res. 5 (6) (2017) 1–6.
[42] S. Jaworski, E. Sawosz, M. Grodzik, M. Kutwin, M. Wierzbicki, K. Włodyga, A. Jasik, M. Reichert, A. Chwalibog, Comparison of tumour morphology and structure from U87 and U118 glioma cells cultured on chicken embryo chorioallantoic membrane, J. Vet. Res. 57 (4) (2013) 593–598.
[43] R. Dong, B. Guo, Smart wound dressings for wound healing, Nano Today 41 (2021), 101290.